ORIGINAL PAPER

Multi-stage image registration based on list-mode proton radiographies for small animal proton irradiation: A simulation study

Prasannakumar Palaniappan [*], **Yana Knudsen, Sebastian Meyer** [†], **Chiara Gianoli, Katrin Schnürle, Matthias Würl, Jonathan Bortfeldt, Katia Parodi** [‡], **Marco Riboldi** [‡]

Department of Medical Physics – Experimental Physics, Ludwig-Maximilians-Universität München, Munich, Germany

Received 21 September 2022; accepted 3 April 2023

Abstract

We present a multi-stage and multi-resolution deformable image registration framework for image-guidance at a small animal proton irradiation platform. The framework is based on list-mode proton radiographies acquired at different angles, which are used to deform a 3D treatment planning CT relying on normalized mutual information (NMI) or root mean square error (RMSE) in the projection domain.

We utilized a mouse X-ray micro-CT expressed in relative stopping power (RSP), and obtained Monte Carlo simulations of proton images in list-mode for three different treatment sites (brain, head and neck, lung). Rigid transformations and controlled artificial deformation were applied to mimic position misalignments, weight loss and breathing changes. Results were evaluated based on the residual RMSE of RSP in the image domain including the comparison of extracted local features, i.e. between the reference micro-CT and the one transformed taking into account the calculated deformation.

The residual RMSE of the RSP showed that the accuracy of the registration framework is promising for compensating rigid (>97% accuracy) and non-rigid (∼95% accuracy) transformations with respect to a conventional 3D-3D registration. Results showed that the registration accuracy is degraded when considering the realistic detector performance and NMI as a metric, whereas the RMSE in projection domain is rather insensitive.

This work demonstrates the pre-clinical feasibility of the registration framework on different treatment sites and its use for small animal imaging with a realistic detector. Further computational optimization of the framework is required to enable the use of this tool for online estimation of the deformation.

Keywords: Image-guidance; Image Registration; Small animal proton irradiation; Pre-clinical; Proton radiographies

Introduction

Small animal pre-clinical *in vivo* irradiation studies are crucial for the translation of radiobiological research into future clinical practice [1]. Radiobiological investigations require the availability of onboard image guidance, aiming at accurate setup and monitoring of anatomical changes. This is currently commercially available for photon-based small animal irradiation, with dedicated experimental platforms where image guidance technologies have been integrated [26]. In this context, 3D Deformable Image registration (DIR) has been used to quantify and compensate

* Corresponding author: Prasannakumar Palaniappan, Department of Medical Physics – Experimental Physics, Ludwig-Maximilians-Universität München, Munich, Germany.

E-mail: P.Palaniappan@physik.uni-muenchen.de (P. Palaniappan).

† Present address: Department of Medical Physics, Memorial Sloan Kettering Cancer Center, New York, NY, USA.

‡ These authors contributed equally to this work.

Z Med Phys **xxx** (2023) xxx–xxx
https://doi.org/10.1016/j.zemedi.2023.04.003
www.elsevier.com/locate/zemedi

anatomical changes in the lung over the irradiation period, relying on the integrated micro-CT imaging device [27]. The use of commercial DIR solutions for multimodal image registration has also been proposed, in order to provide MRI-based planning in small animal experiments [2]. More advanced imaging modalities, such as CBCT at different energies [3], bioluminescence and fluorescent tomography [4] and radioluminescence imaging [5] are also under investigation for photon-based irradiation.

Different groups have proposed and integrated an existing image guidance device for small animals, designed for photon irradiation, into a proton beamline [6,7], which has only recently led to the availability of a commercial solution. The interest towards such studies has been growing due to the ongoing research efforts concerning FLASH [8,9], proton mini-beam irradiation [10] and in addition to remaining open questions concerning the in-vivo assessment of relative biological effectiveness. A dedicated platform for small animal proton irradiation has been developed in the framework of the "Small animal proton irradiator for research in molecular image-guided radiation-oncology (SIRMIO)" project [28]. The platform is portable, and includes a system for energy degradation and active focusing of clinical proton beams [11], a motorized mouse holder as well as integrated imaging devices [33].

The steep dose gradients and the overall sensitivity to range uncertainties in proton therapy call for even more advanced image guidance methods, even at the pre-clinical stage. The proton range is determined from treatment planning CT images via a stoichiometric conversion of Hounsfield units (HU) values into the required ion relative stopping power (RSP) [12]. This approach yields uncertainties around 3% of the range in clinical applications [13], which are further emphasized in pre-clinical use by the fact that human reference data are used for dose calculations [14]. Proton Computed Tomography (pCT) is a potential replacement to a semi-empirically calibrated treatment planning CT [16,17]. The superiority of pCT over conventional CT has been demonstrated using simulation and in experimental studies for clinically oriented proton imaging prototypes or ideal detectors [18,19]. The water equivalent thickness (WET) measured as the integral RSP in list-mode proton radiographies (pRads) in projection space is used in pCT tomographic reconstruction [20,21]. In single particle tracking detectors, trackers positioned before and after object of interest are used to estimate the trajectory of each individual proton [22,23]. A range telescope enclosed with a series of absorption layers with interleaved detection layers or a single or segmented calorimeter is able to measure the residual energy [24,25]. The range is then calibrated to WET relying on a dedicated calibration procedure. A similar concept has been extended to small animals in the SIRMIO project, relying on low-material budget gas detectors to overcome the issues of enhanced scattering at the requested low energies for small animal imaging [33].

In this study, we investigate the performance of registration [29,30] based on list-mode proton radiographies of a small-animal to provide (i) a setup correction vector to account for position misalignments and (ii) a deformation field to quantify anatomical changes. For this purpose, we extended the framework to a multi-stage multi-resolution implementation of the registration algorithm, which has been specifically developed to handle both transformations. Previous studies were restricted only to an ideal detector, whereas in this work the realistic detector conditions were explored. The list-mode proton radiographies were obtained based on the Monte Carlo (MC) simulations considering a detailed model of the detector developed for the SIRMIO platform [33]. Rigid transformations and combination of both rigid and artificial anatomical changes were applied to the treatment planning CT of three treatment sites imitating the position misalignment, weight loss and breathing changes in the in-situ proton irradiation. The local features were extracted using the scale-invariant feature transform (SIFT) between the volumes prior to and after registration for accuracy quantification.

Methods and materials

Monte Carlo simulation framework and small animal imaging

We used an X-ray micro-CT image, which was downsampled from 0.103 mm to a 0.2 mm isotropic voxel spacing, relying on cubic-spline interpolation. Three different treatments sites, brain, head & neck (H&N) and lung were considered for a hypothetical tumor treatment. For all investigated treatment sites, the axial field of view was set to 10 slices (2 mm). The reference ground truth pCT was initially obtained by relying on a calibration curve mapping the HU values of the micro-CT to RSP. Later, this ground truth pCT expressed in RSP was used for all the investigated registration scenarios and also used as input geometry in FLUKA based MC simulations [31,32] of pRads for the single particle tracking (list-mode) detector considering the geometrical and optimized realistic SIRMIO pCT detector model [33]. The system is based on cost efficient in house-developed Micromegas gaseous detectors and a Time Projection Chamber with multiple Mylar absorbers functioning as a range telescope to measure the residual range of each individual protons [34]. The residual range was expressed in terms of water equivalent path length (WEPL). Based on previous investigations [33] on the optimal trade-off between WEPL resolution and detector complexity, a 500 μm absorber thickness was selected in this work. The experimental beam characteristics of the ProBeam line (Varian Medical systems,

Please cite this article as: P. Palaniappan, Y. Knudsen, S. Meyer et al., Multi-stage image registration based on list-mode proton radiographies for small animal proton irradiation: A simulation study, Z Med Phys, https://doi.org/10.1016/j.zemedi.2023.04.003

USA) were used for scanned proton beams at the nominal energy of 75 MeV [35] and with the dose exposure of (93 ±5) mGy. The effective spatial resolution was modelled by adding a random normal uncertainty with $\sigma = 80$ μm to the obtained lateral position values [33]. In addition to the real detector model, an ideal pCT detector system is considered for the brain case. In the ideal model, the scoring planes monitoring the direction, position and energy of each proton prior to and after the treatment site were considered, assuming perfect detection. The pRads uniformly covered 180° angular range in nine separate list mode proton radiographies (in projection space). In addition, the lateral pRad (at 0°) complementing the frontal one (at 90°) is considered, therefore taking full advantage of orthogonality between pRads. The geometrical parameters of the performed MC simulations are reported in Table 1. Based on 180 projections (2° of spacing covering 360°) a volumetric pCT is reconstructed relying on the iterative ordered-subset simultaneous algebraic reconstruction method [36] incorporated with total variation superiorization [37], considering a straight-line path through the mouse for each proton.

Multi-stage multi-resolution registration and investigated scenarios

Relying on the results from previous findings in clinical-like scenarios [29,30] the registration framework was extended to a multi-stage multi-resolution registration framework. A limited memory quasi-Newton Broyden-Fletcher-Goldfarb-Shanno optimization algorithm, commonly employed in 3D-3D DIR, is adopted as the optimization algorithm [15]. A single-stage rigid image registration (RIR) is carried out explicitly to mimic the position misalignments. In the multi-stage registration, the initial stage is dedicated to compensate the rigid component of the mismatch, whereas the subsequent stages include a deformable transform to account for non-rigid changes. Utilizing the transformation matrix from the first stage, a free form deformation based on cubic basis splines (B-splines) is implemented. For rigid transformations, three sets of random displacements were selected as shown in Table 2, where the treatment planning CT expressed in RSP for all sites was first translated in a range of [−2.4, 2.4] mm and followed by a rotation in a range of [−5°, 5°] along the latero-lateral and cranio-caudal directions. For non-rigid transformations, an artificial Gaussian in each direction of the deformation field with an amplitude and standard deviation of 1 mm and 2 mm respectively was considered for brain and H&N site, as shown in Table 3. The deformation fields are laterally placed at different locations to imitate a realistic weight loss in brain and H&N sites. For the most complex lung treatment site, three sets of random transformation were chosen as shown in Table 4. The radial expansion with a random displacement magnitude in the range of [−2, 2] mm in the cranio-caudal direction was applied in the lung site to mimic breathing motion. The radial expansion field was applied on both sides of the lung, approximately positioned at the top of the diaphragm. A random Gaussian transform with standard deviation in the [−2, 2] mm range and [−1, 1] mm amplitude along the three directions was additionally applied to mimic weight loss. The vector field including the combined anatomical changes was then warped together with the rigid transformations to obtain the combination of rigid and non-rigid transformations (Table 3 and Table 4).

In the multi-stage registration, the number of iterations was set equal to 15 for the first rigid stage and to 15 and 10 iterations for the next two multi-resolution (with grid spacing corresponding to 32 and 16 voxels) deformable registration stages, respectively. The objective function of the optimization was either the root mean square error (RMSE) or the normalized mutual information (NMI) between the fixed list-mode proton radiographies and the forward projection of the moving treatment planning CT [29]. The accuracy of the registration was quantified using translation and rotation recovered in RIR. In addition, the RMSE of RSP (intensity-based in image domain) between the ground truth pCT (including air) and the moving image was calculated in both RIR and DIR. Relying on the same registration parameters, the performance of the registration was evaluated in comparison to a conventional 3D-3D registration. The 3D-

Table 1
Geometrical parameters adopted in MC simulations.

Geometrical parameters			
Treatment site	Brain	H&N	Lung
Detector model	Realistic, ideal	Realistic	Realistic
Slice thickness	2 mm		
Image size	20.1 × 20.1 mm^2	20.1 × 20.1 mm^2	25.5 × 25.5 mm^2
Number of slices	10		
Rad angles	0°, 90° (2 pRads)		
	10°, 30°, 50°, 70°, 90°, 110°, 130°, 150°, 170° (9 pRads)		

Please cite this article as: P. Palaniappan, Y. Knudsen, S. Meyer et al., Multi-stage image registration based on list-mode proton radiographies for small animal proton irradiation: A simulation study, Z Med Phys, https://doi.org/10.1016/j.zemedi.2023.04.003

Table 2
Applied translation and rotation by random selection of rigid motion.

Site	Brain		H & N		Lung	
	Translation (mm)	Rotation (deg)	Translation (mm)	Rotation (deg)	Translation (mm)	Rotation (deg)
Rigid motion 1	−1.06	4.64°	1.51	4.13°	0.18	−0.57°
Rigid motion 2	0.22	−3.42°	1.94	1.32°	2.38	−3.93°
Rigid motion 3	2.19	4.7°	−1.79	−4.02°	−2.02	4.61°

Table 3
Applied combination of rigid and non-rigid transformation to brain and H&N site.

Site	Rigid		Non-rigid
	Translation	Rotation	Gaussian (amplitude, std deviation)
Brain, H & N	1.2mm	5°	1mm, 2 mm

Table 4
Applied combination of rigid and non-rigid transformation to the lung site.

Site	Rigid		Non-rigid	
	Translation	Rotation	Gaussian (amplitude, std deviation)	Radial expansion (magnitude)
Transformation 1			0.83mm, 1.66mm	1.66mm
Transformation 2	2.38 mm	−3.93°	−0.46mm, −0.92mm,	−0.92 mm
Transformation 3			0.531mm, 1.06mm	1.06mm

3D registration was carried out between the treatment planning CT expressed in RSP as moving image and the reconstructed pCT (RpCT) from the employed detector model as the fixed image. Relying on the SIFT transform [38] the local features were extracted and matched to quantify the registration accuracy [39,40]. The mean square error (MSE) of the matched features between the two sets i.e., (i) ground truth pCT and moving image (prior to registration) and (ii) ground truth pCT and image after registration were calculated in brain site.

Results

Rigid registration

The rigid registration is able to recover the applied rotation and translation using 2 or 9 pRads (both similarity metrics) in brain, H&N and lung treatment sites based on realistic detectors and including the ideal detector (brain site). The residual RMSE of RSP with respect to number of iterations are reported in Appendix (Figs. A1 and A2). A small difference in the intensity-based quantification (RMSE of RSP) is observed when compensating the rigid motions using RpCT in 3D-3D registration between the ideal and realistic detector, but it does not reflect the obtained accuracy in RIR (Fig. A1). This difference is further minimized in H&N and Lung sites (Fig. A2).

Non-rigid registration

The intensity-based quantification (difference in RMSE of RSP prior to and after all stages) when compensating the applied combination of rigid and non-rigid transformations in the brain site from realistic and ideal detector models using 2 pRads and 9 pRads is shown in the Fig. 1(A) and (B), respectively. The compensation of the applied transformations for H&N and lung sites from the realistic detector model is shown in Figs. 2 and 3, respectively. In all three sites, the registration using 9 pRads is able to keep up with the similar accuracy as the conventional 3D-3D registration provided with the same registration parameters, whereas the 2 pRads remain slightly inferior. A slightly improved accuracy is observed for the RMSE metric over NMI for all the three-treatment site. The convergence of corresponding RMSE of RSP at each iteration for brain, H&N and lung site is shown in Figs. 4 and 5. The obtained SIFT features are visualized in Fig. 6, including the MSE of the SIFT feature coordinates which correlates to the accuracy of the registration for both ideal and realistic detectors for brain site.

Please cite this article as: P. Palaniappan, Y. Knudsen, S. Meyer et al., Multi-stage image registration based on list-mode proton radiographies for small animal proton irradiation: A simulation study, Z Med Phys, https://doi.org/10.1016/j.zemedi.2023.04.003

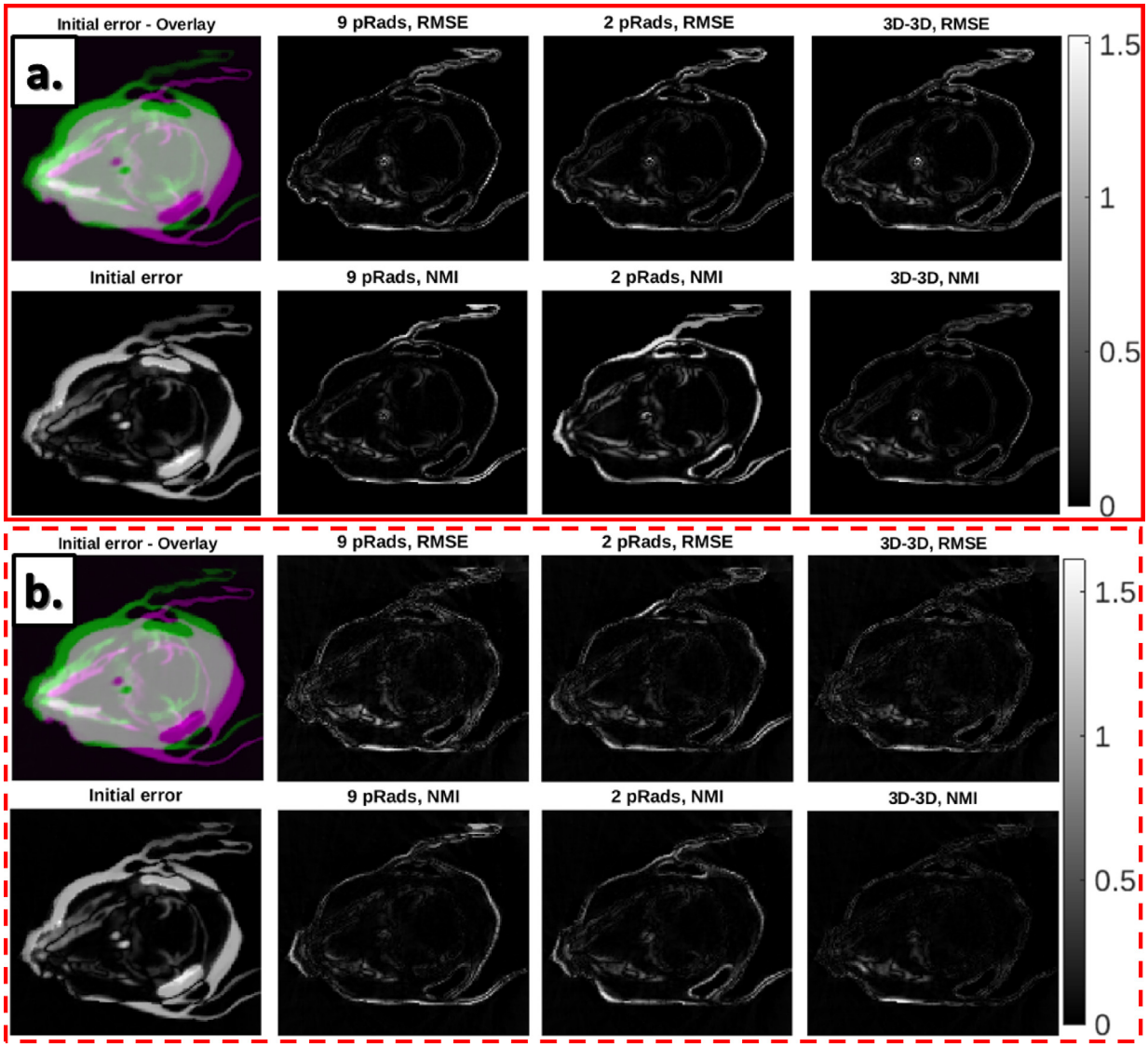

Figure 1. Intensity based quantification (RMSE of RSP) of the ground truth pCT and the calibrated treatment planning CT for the brain, prior to (initial error) and after (for different metrics) multi-stage registration using 9 and 2 pRads to compensate the combination of rigid and non-rigid transformations. Panels (A) show the results for the realistic detector model, whereas panels (B) refers to the ideal detector. Conventional 3D-3D registration with fixed image as RpCT is also included.

Discussions

A multi-stage registration framework was designed to exploit list mode proton radiographies in a small animal irradiation platform to calculate setup corrections and anatomical deformation. The framework extends previous implementation of the algorithm that was investigated on an anthropomorphic phantom [29] and clinical data from H&N patients [30]. This study is therefore the first application of the algorithm to small animal imaging, and the general framework was re-designed to account for rigid registration followed by deformation compensation. Unlike previous studies, which relied on ideal detector conditions, here we demonstrate the applicability of the framework to the data from a realistic detector simulations of a prototype small animal imager [33]. The rigid motions (i.e. applied rotation and translation in Table 2) were accurately recovered (97% - 99% in terms of recovered translation in “mm” and rotation in degrees) for both 2D-3D and 3D-3D RIR. However, the RMSE of RSP of 3D-3D RIR is slightly inferior to the 2D-3D RIR (Figs. A1 and A2) in all sites denoting the influence of RpCT image

Please cite this article as: P. Palaniappan, Y. Knudsen, S. Meyer et al., Multi-stage image registration based on list-mode proton radiographies for small animal proton irradiation: A simulation study, Z Med Phys, https://doi.org/10.1016/j.zemedi.2023.04.003

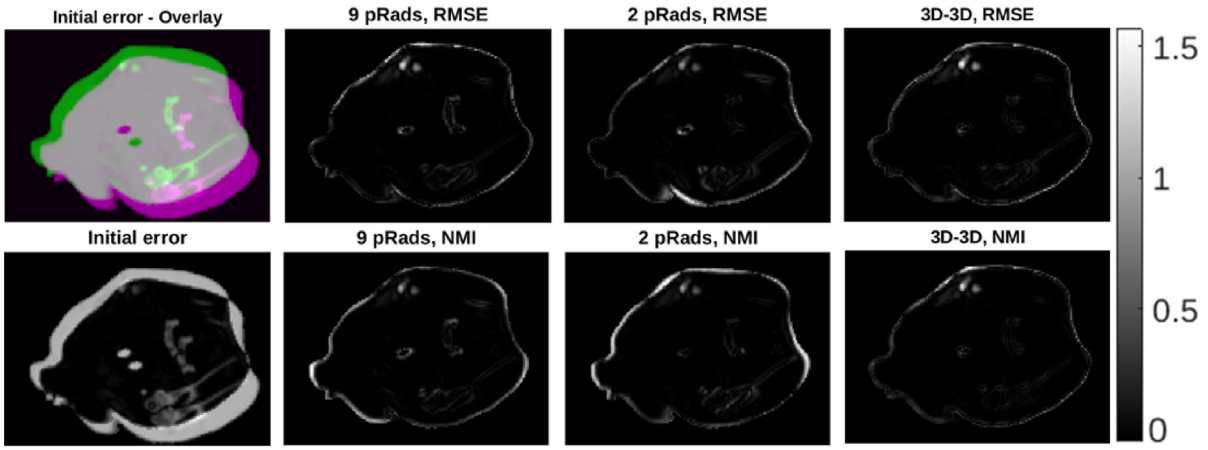

Figure 2. Intensity based quantification (RMSE of RSP) of the ground truth pCT and the calibrated treatment planning CT for H&N site.

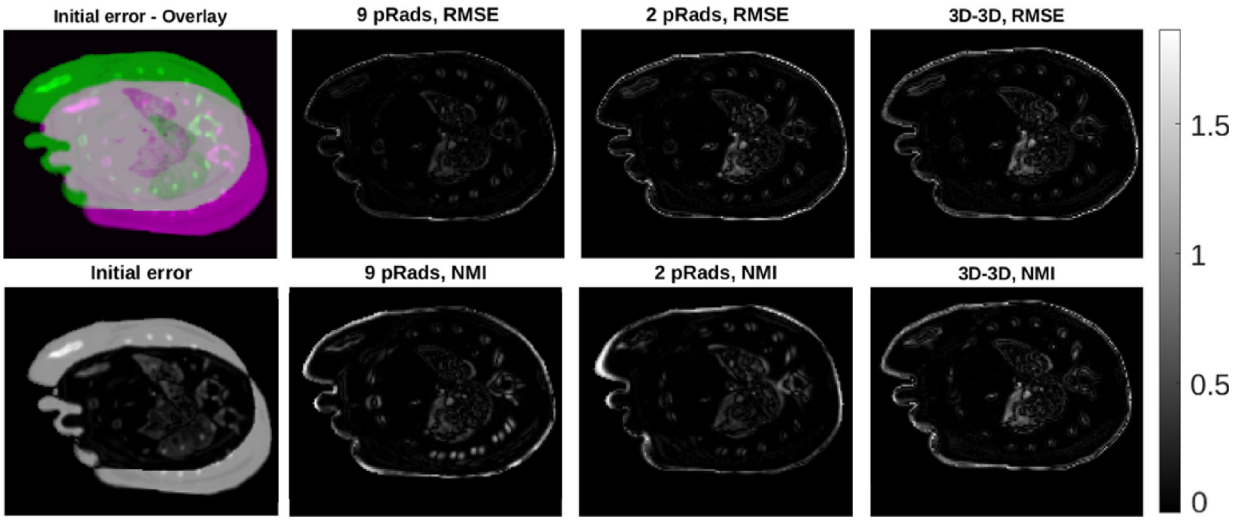

Figure 3. Intensity based quantification (RMSE of RSP) of the ground truth pCT and the calibrated treatment planning CT in lung site for applied 'transformation 2' from Table 4.

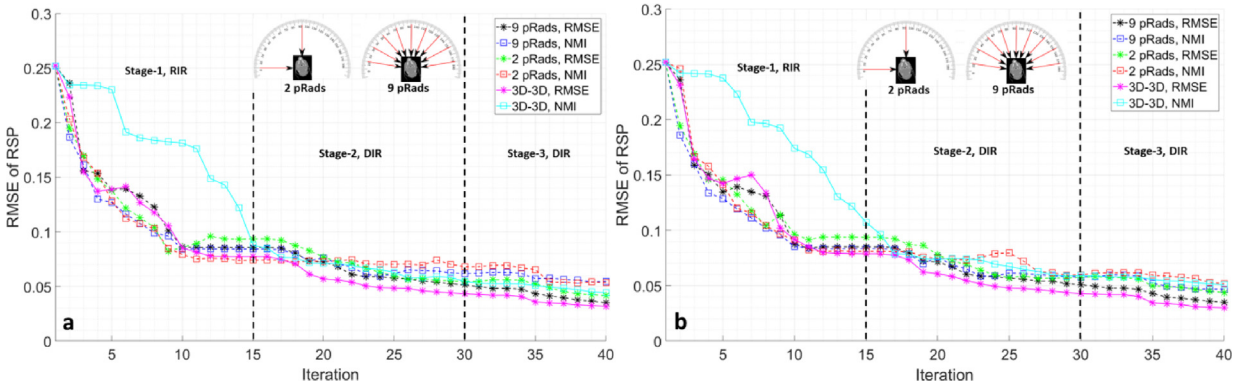

Figure 4. Evaluation of intensity-based quantification compensating the combination of rigid and non-rigid transformations in brain site by using 9 and 2 pRads for realistic detector (a) and ideal detector (b) configuration, including the conventional 3D-3D registration with fixed image as RpCT.

Please cite this article as: P. Palaniappan, Y. Knudsen, S. Meyer et al., Multi-stage image registration based on list-mode proton radiographies for small animal proton irradiation: A simulation study, Z Med Phys, https://doi.org/10.1016/j.zemedi.2023.04.003

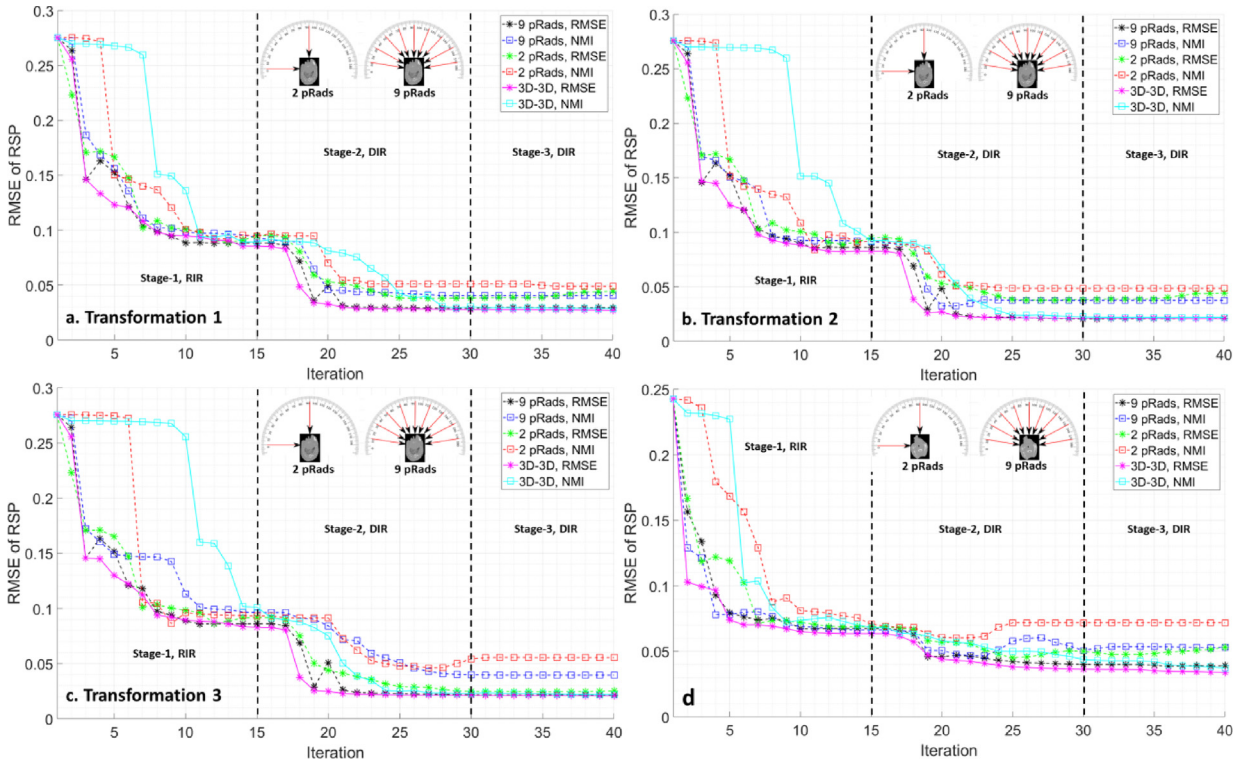

Figure 5. Evaluation of intensity-based quantification compensating the combination of rigid and non-rigid transformation sets (a, b, c) reported in Table 4 in lung and H&N (d) site.

quality as fixed image in 3D-3D RIR. Such a difference did not penalize the ability of the algorithm to recover the applied rigid transformation, despite the small difference in RMSE of RSP values. When compensating the combination of rigid and non-rigid changes using RMSE as a similarity metric (radiographic domain), the multi-stage and multi-resolution registration framework achieved similar performance compared to 3D-3D registration. In the brain images for the realistic detector, a residual RMSE of RSP equal to 0.0340 and 0.0405 was achieved for 9 pRads and 2 pRads, respectively, vs. 0.0312 for 3D-3D registration. Using the NMI as a metric proved to be inferior: the RMSE of RSP for the brain site and realistic detector was 0.0541, 0.0537 and 0.0401 for 9 pRads, 2 pRads and 3D-3D registration, respectively. The feasibility of the registration was further investigated by random selection for both Rigid and combination of rigid and non-rigid transformations. The feature-based metric in image domain, i.e. the MSE of the SIFT features, suggests significant improvements in terms of registration accuracy. Especially the behavior of the worst performing 2 pRads NMI is comparable to the intensity-based quantification (RMSE of RSP) in Fig. 1 (Panel A) for realistic detector, but not necessarily noticeable in the convergence plot in Fig. 4(a). Furthermore, the 3D-3D registration based on RMSE (ideal detector) achieves the best accuracy (lowest SIFT error), thus indicating that the image quality of RpCT has a negligible influence on the registration accuracy. The adopted limited memory quasi-Newton Broyden-Fletcher-Goldfarb-Shanno optimization algorithm based on the Newton direction for line search reaches the tolerance value when there is no noticeable local minimum between fixed and moving or the convergence is too small in RIR and reflects in the different number of iterations needed in Fig. A1 and A2.

The computation of RIR at the first stage takes only few minutes but the DIR at later stages especially at finer resolution (16pixel grid spacing) is computationally expensive, thus limiting the number of iterations in the final stages. In previous work [30] the random sampling of objective function was used to improve the computation of the framework with a slight tradeoff to the achievable accuracy. However, a specific optimization of the B-spline transformation and of the analytical calculation of the forward projection using pRads requires an extensive investigation. An additional limitation of our study is that the HU-RSP mapping is kept constant between the reference and moving image, which may fail to consider changes in the calibration curve.

Please cite this article as: P. Palaniappan, Y. Knudsen, S. Meyer et al., Multi-stage image registration based on list-mode proton radiographies for small animal proton irradiation: A simulation study, Z Med Phys, https://doi.org/10.1016/j.zemedi.2023.04.003

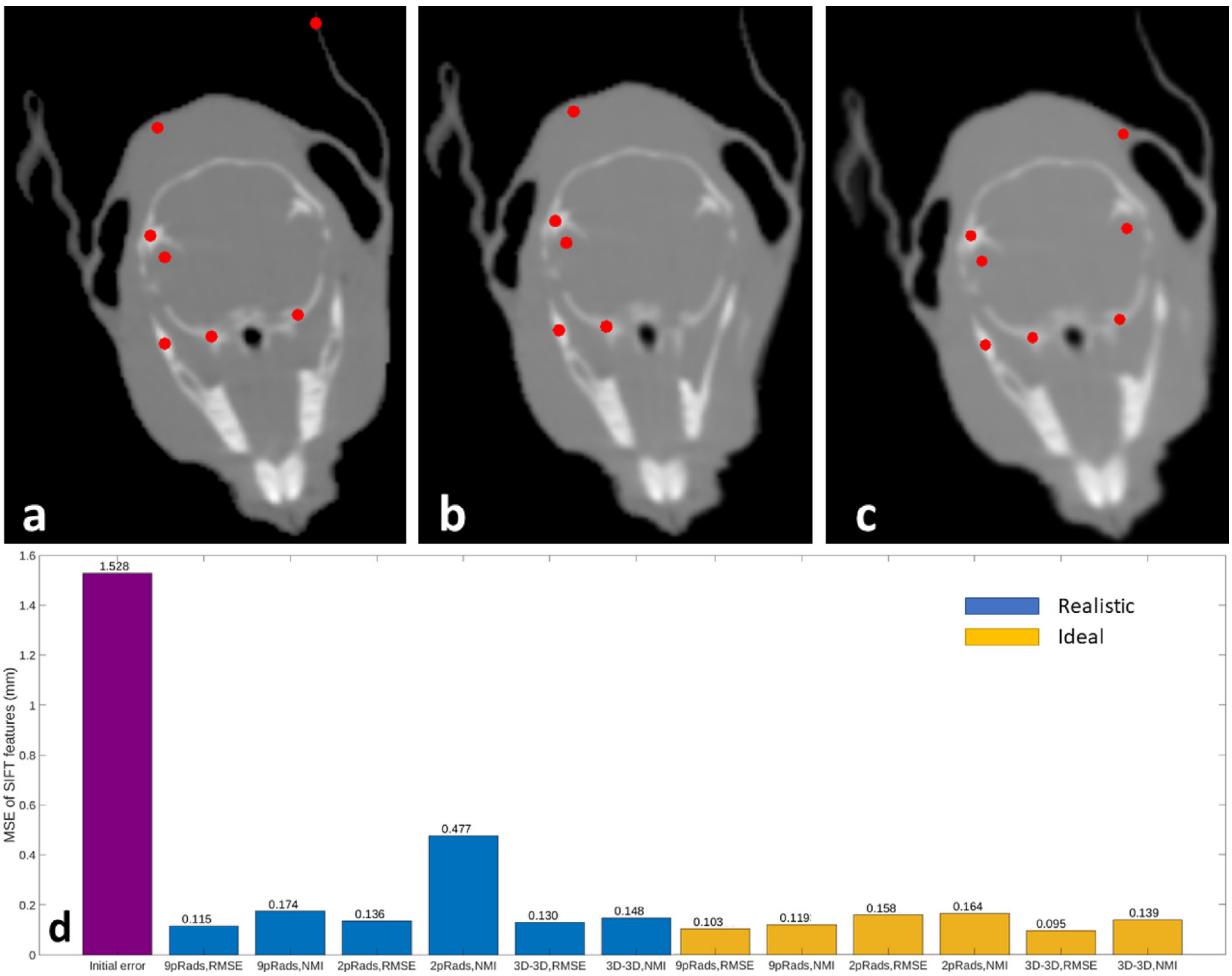

Figure 6. SIFT transform features for reference ground truth pCT expressed in RSP (a), prior to (b), after (c) registration and calculated MSE of SIFT features (d) in brain site.

In future work, the registration framework will be extended to realistic and simplified in-house developed integration-mode detector, which neglects single particle tracking, resulting in an integral (pencil-beam wise) measurement. The choice of metrics will be further investigated based on the superiority of NMI as metric in the previous study considering only the ideal integration mode detector condition [29]. Moreover, the accuracy of registration is expected to degrade for integration mode detectors providing a reduced amount of information with respect to list mode radiographies. Therefore, additional projections in integration mode are required to utilize the full potential of the developed system, aiming at comparable accuracy. In addition, the registration framework could be combined with the optimization of the empirical HU-RSP calibration curve [41], thus enabling a calibration refinement taking into account the calculated anatomical changes.

Conclusion

The implemented registration framework provides accurate results in compensating rigid and non-rigid transformations for data from a realistic simulation model of a small-animal irradiation platform. The current implementation allows for compensation of setup changes online, but requires significant speed-up to provide fast deformation estimation. Further studies involving integration-mode detectors and the joint implementation of (i) registration and (ii) optimization of the calibration curve are needed.

Data Availability Statement

The code used to extract the data is distributed by the authors as open-source. The patient data can be made available on request due to privacy/ethical restrictions.

Please cite this article as: P. Palaniappan, Y. Knudsen, S. Meyer et al., Multi-stage image registration based on list-mode proton radiographies for small animal proton irradiation: A simulation study, Z Med Phys, https://doi.org/10.1016/j.zemedi.2023.04.003

Declaration of Competing Interest

The authors declare that they have no known competing financial interests or personal relationships that could have appeared to influence the work reported in this paper.

Acknowledgements

Dr. Sebastian Meyer, Dr. Chiara Gianoli, Katrin Schnürle, Dr. Matthias Würl, Dr. Jonathan Bortfeldt and Prof. Dr. Katia Parodi acknowledge the project SIRMIO (Small Animal Proton Irradiator for Research in Molecular Image-guided Radiation-Oncology), funded by the European Research Council (ERC) under the European Union's Horizon 2020 research and innovation programme through the Grant Agreement No. 725539. Dr. Chiara Gianoli and Prof. Dr. Katia Parodi also acknowledge the Deutsche Forschungsgemeinschaft (DFG) project "Hybrid imaging framework in hadrontherapy for adaptive radiation therapy", grant#372393016. Dr. Prasannakumar Palaniappan and Prof. Dr. Marco Riboldi acknowledge the DFG project 'Radiography driven deformable image registration in adaptive proton therapy', grant#455550444. Furthermore, the authors thank Prof. Frank Verhaegen for providing the mouse CT data.

Appendix

(Figs. A1 and A2)

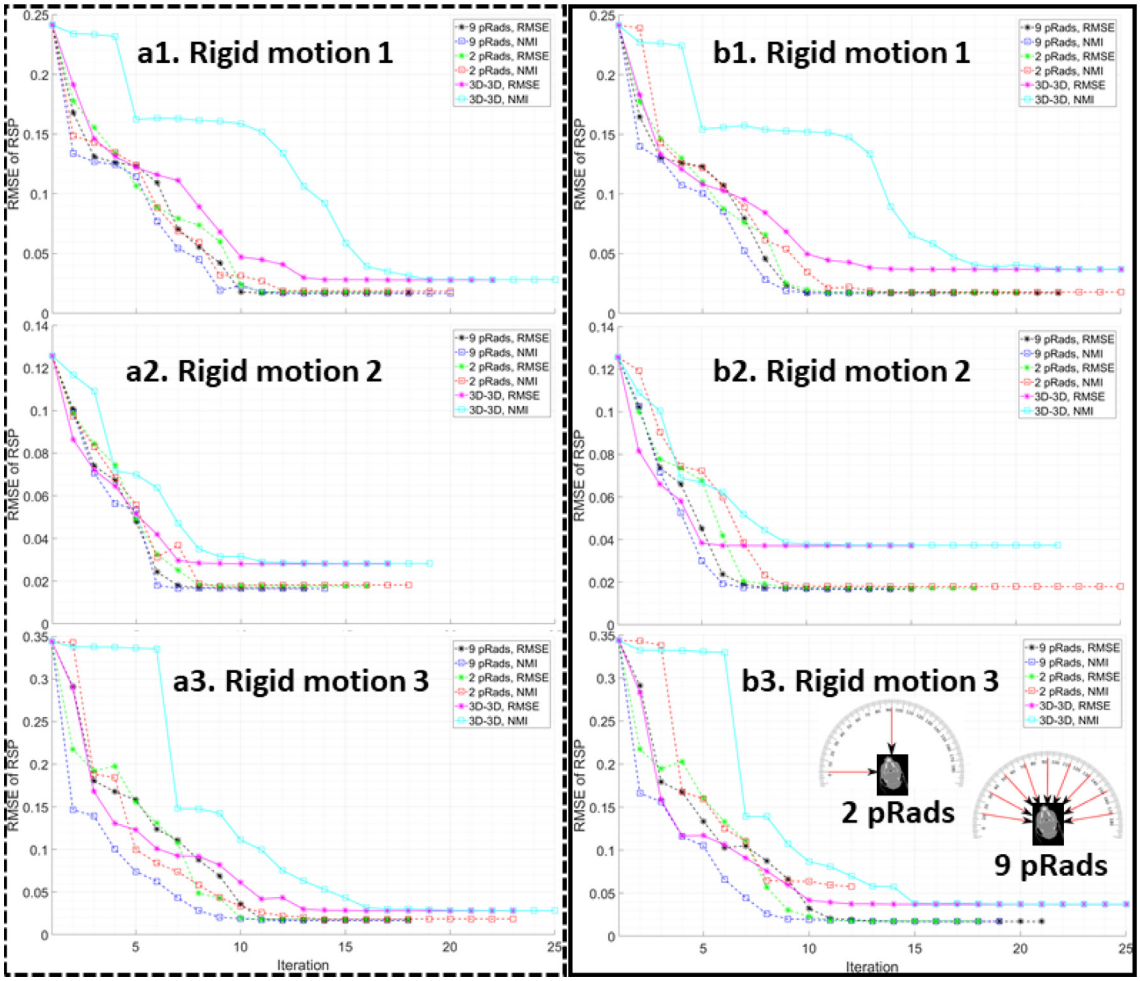

Figure A1. Evaluation of intensity-based quantification compensating the rigid changes in brain site using the ideal detector (a1, a2, a3) and realistic detector (b1, b2, b3), including the conventional 3D-3D registration with fixed image as RpCT.

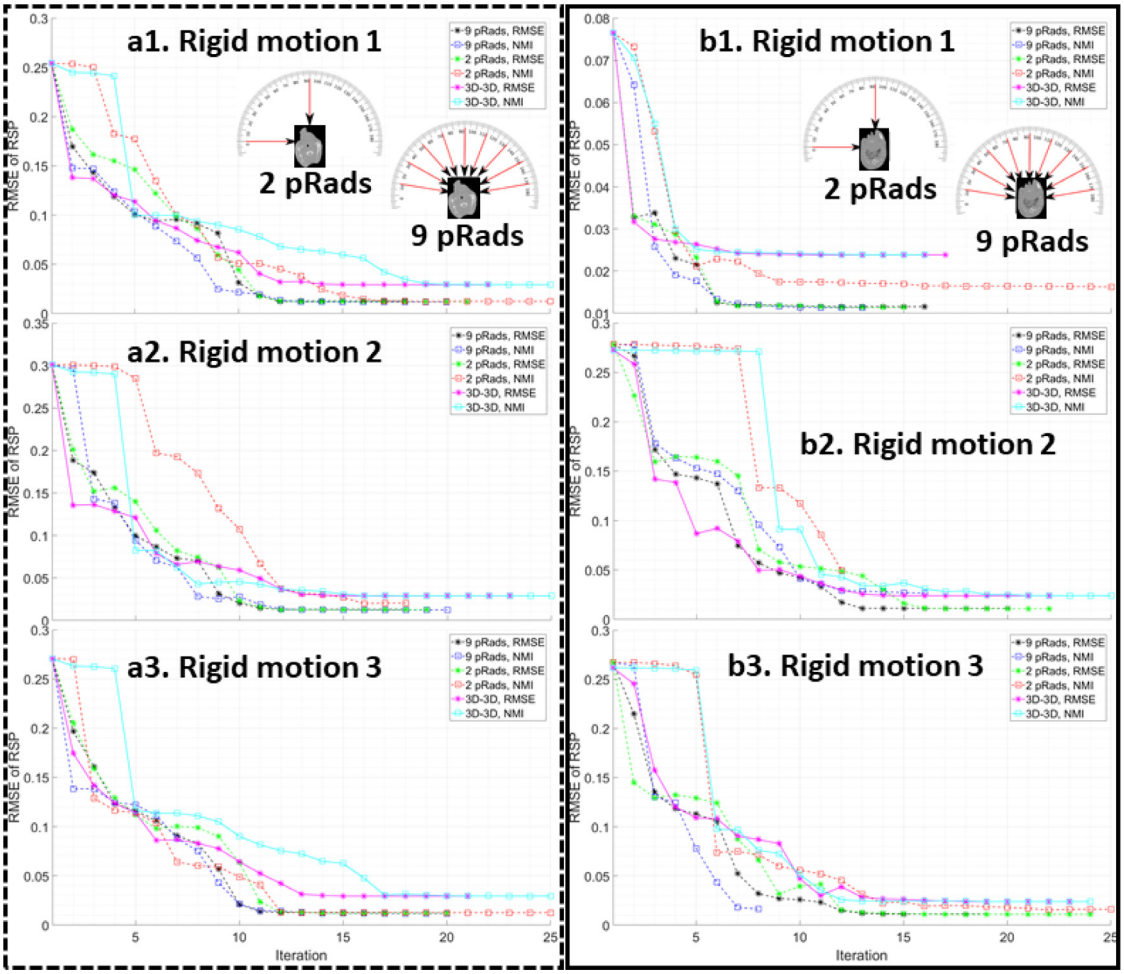

Figure A2. Evaluation of intensity-based quantification compensating the rigid changes in H&N (a1, a2, a3) and lung (b1, b2, b3) sites using the realistic detector, including the conventional 3D-3D registration with fixed image as RpCT.

References

[1] Brown KH, Ghita M, Dubois LJ, de Ruysscher D, Prise KM, Verhaegen F, Butterworth KT. A scoping review of small animal image-guided radiotherapy research: Advances, impact and future opportunities in translational radiobiology. Clin Transl Radiat Oncol 2022;6(34):112–119. https://doi.org/10.1016/j.ctro.2022.04.004.

[2] Black PJ, Smith DR, Chaudhary K, Xanthopoulos EP, Chin C, Spina CS, Hwang ME, Mayeda M, Wang YF, Connolly EP, Wang TJC, Wuu CS, Hei TK, Cheng SK, Wu CC. Velocity-based Adaptive Registration and Fusion for Fractionated Stereotactic Radiosurgery Using the Small Animal Radiation Research Platform. Int J Radiat Oncol Biol Phys 2018;102(4):841–847. https://doi.org/10.1016/j.ijrobp.2018.04.067.

[3] Huang Y, Hu X, Zhong Y, Lai Y, Shen C, Jia X. Improving dose calculation accuracy in preclinical radiation experiments using multi-energy element resolved cone-beam CT. Phys Med Biol 2021;66(24). https://doi.org/10.1088/1361-6560/ac37fc.

[4] Shi J, Xu K, Keyvanloo A, Udayakumar TS, Ahmad A, Yang F, Yang Y. A Multimodality Image Guided Precision Radiation Research Platform: Integrating X-ray, Bioluminescence, and Fluorescence Tomography With Radiation Therapy. Int J Radiat Oncol Biol Phys 2020;108(4):1063–1072. https://doi.org/10.1016/j.ijrobp.2020.06.023.

[5] Spinelli AE, D'Agostino E, Broggi S, Claudio F, Boschi F. Small animal irradiator dose distribution verification using radioluminescence imaging. J Biophotonics 2020;13(7):e201960217. https://doi.org/10.1002/jbio.201960217.

[6] Ford E, Emery R, Huff D, Narayanan M, Schwartz J, Cao N, Meyer J, Rengan R, Zeng J, Sandison G, Laramore G, Mayr N. An image-guided precision proton radiation platform for preclinical in vivo research. Phys Med Biol 2017;62(1):43–58. https://doi.org/10.1088/1361-6560/62/1/43.

[7] Kim MM, Irmen P, Shoniyozov K, Verginadis II, Cengel KA, Koumenis C, Metz JM, Dong L, Diffenderfer ES. Design and commissioning of an image-guided small animal radiation platform and quality assurance protocol for integrated proton and x-ray

radiobiology research. Phys Med Biol 2019;64(13):135013. https://doi.org/10.1088/1361-6560/ab20d9.

[8] Patriarca A, Fouillade C, Auger M, Martin F, Pouzoulet F, Nauraye C, Heinrich S, Favaudon V, Meyroneinc S, Dendale R, Mazal A, Poortmans P, Verrelle P, De Marzi L. Experimental Set-up for FLASH Proton Irradiation of Small Animals Using a Clinical System. Int J Radiat Oncol Biol Phys 2018;102(3):619–626. https://doi.org/10.1016/j.ijrobp.2018.06.403.

[9] Grilj V, Buonanno M, Welch D, Brenner DJ. Proton Irradiation Platforms for Preclinical Studies of High-Dose-Rate (FLASH) Effects at RARAF. Radiat Res 2020;194(6):646–655. https://doi.org/10.1667/RADE-20-00062.1.

[10] Bertho A, Ortiz R, Juchaux M, Gilbert C, Lamirault C, Pouzoulet F, Polledo L, Liens A, Warfving N, Sebrie C, Jourdain L, Patriarca A, de Marzi L, Prezado Y. First Evaluation of Temporal and Spatial Fractionation in Proton Minibeam Radiation Therapy of Glioma-Bearing Rats. Cancers (Basel) 2021;13(19):4865. https://doi.org/10.3390/cancers13194865.

[11] Gerlach S, Pinto M, Kurichiyanil N, Grau C, Hérault J, Hillbrand M, Poulsen PR, Safai S, Schippers JM, Schwarz M, Søndergaard CS, Tommasino F, Verroi E, Vidal M, Yohannes I, Schreiber J, Parodi K. Beam characterization and feasibility study for a small animal irradiation platform at clinical proton therapy facilities. Phys Med Biol 2020;65(24):245045.

[12] Schneider U, Pedroni E, Lomax A. The calibration of CT Hounsfield units for radiotherapy treatment planning. Phys Med Biol 1996;41(1):111–124. https://doi.org/10.1088/0031-9155/41/1/009.

[13] Yang M, Zhu XR, Park P, Titt U, Mohan R, Virshup G, Clayton J, Dong L. Comprehensive analysis of proton range uncertainties related to patient stopping-power-ratio estimation using the stoichiometric calibration. Phys Med Biol 2012;57:4095–4115.

[14] Schyns LEJR, Eekers DBP, van der Heyden B, Almeida IP, Vaniqui A, Verhaegen F. Murine vs human tissue compositions: implications of using human tissue compositions for photon energy absorption in mice. Brit J Radiol 2019;92:20180454.

[15] Dennis Jr JE, More J. Quasi-Newton methods, motivation and theory. SIAM Rev 1977;19:46–89.

[16] Parodi K. Heavy ion radiography and tomography. Physica medica 2014;30(5):539–543.

[17] Johnson RP. Review of medical radiography and tomography with proton beams. Rep Prog Phys 2017;81(1):016701.

[18] Dedes G, Dickmann J, Niepel K, Wesp P, Johnson RP, Pankuch M, Bashkirov V, Rit S, Volz L, Schulte RW, Landry G, Parodi K. Experimental comparison of proton CT and dual energy x-ray CT for relative stopping power estimation in proton therapy. Phys Med Biol 2019;64:165002.

[19] Meyer S, Kamp F, Tessonnier T, Mairani A, Belka C, Carlson DJ, Parodi K. Dosimetric accuracy and radiobiological implications of ion computed tomography for proton therapy treatment planning. Phys Med Biol 2019;64(12):125008.

[20] Gianoli C, Fattori G, Riboldi M, Rinaldi I, Dedes G, Parodi K and Baroni G 2014 Projection-based deformable registration for tomographic imaging in ion beam therapy Nuclear Science Symp. and Medical Imaging Conf. (NSS/MIC). IEEE; 2014. p 1–4.

[21] Gianoli C, Dedes G, Meyer S, Magallanes L, Landry G, Nijhuis R, Parodi K. PO-0909: Merging proton radiographies with treatment planning CT for adaptive radiation therapy. Radiother Oncol 2016;119:S438.

[22] Schulte RW, Penfold SN, Tafas JT, Schubert KE. A maximum likelihood proton path formalism for application in proton computed tomography. Med Phys 2008;35:4849–4856.

[23] Schneider U, Pemler P, Besserer J, Pedroni E, Lomax A, Kaser-Hotz B. Patient specific optimization of the relation between CT-Hounsfield units and proton stopping power with proton radiography. Med Phys 2005;32(1):195–199.

[24] Krah N, De Marzi L, Patriarca A, Pittá G, Rinaldi I. Proton radiography with a commercial range telescope detector using dedicated post processing methods. Phys Med Biol 2018;63(20):205016.

[25] Pettersen HE, Alme J, Biegun A, Van Den Brink A, Chaar M, Fehlker D, Meric I, Odland OH, Peitzmann T, Rocco E, Ullaland K. Proton tracking in a high-granularity Digital Tracking Calorimeter for proton CT purposes. Nucl Instrum Methods Phys Res Sect A: Accelerat, Spectromet, Detectors Assoc Equip 2017;11(860):51–61.

[26] Verhaegen F, Dubois L, Gianolini S, Hill MA, Karger CP, Lauber K, Prise KM, Sarrut D, Thorwarth D, Vanhove C, Vojnovic B. ESTRO ACROP: Technology for precision small animal radiotherapy research: Optimal use and challenges. Radiotherapy Oncol 2018;126(3):471–478.

[27] Granton PV, Dubois L, van Elmpt W, van Hoof SJ, Lieuwes NG, De Ruysscher D, Verhaegen F. A longitudinal evaluation of partial lung irradiation in mice by using a dedicated image-guided small animal irradiator. Int J Radiat Oncol Biol Phys 2014;90(3):696–704.

[28] Parodi K, Assmann W, Belka C, Bortfeldt J, Clevert DA, Dedes G, Kalunga R, Kundel S, Kurichiyanil N, Lämmer P, Lascaud J. Towards a novel small animal proton irradiation platform: the SIRMIO project. Acta Oncol 2019;58(10):1470–1475.

[29] Palaniappan P, Meyer S, Kamp F, Belka C, Riboldi M, Parodi K, Gianoli C. Deformable image registration of the treatment planning CT with proton radiographies in perspective of adaptive proton therapy. Phys Med Biol 2021;66(4):045008.

[30] Palaniappan P, Meyer S, Rädler M, Kamp F, Belka C, Riboldi M, Parodi K, Gianoli C. X-ray CT adaptation based on a 2D–3D deformable image registration framework using simulated in-room proton radiographies. Phys Med Biol; 2022.

[31] Ferrari A, Sala P, Fass'o A, Ranft J. FLUKA: a multi-particle transport code Technical report CERN-2005-10 (2005). INFN/TC 2005;05/11:SLAC-R-773.

[32] Böhlen T et al.. The FLUKA code: developments and challenges for high energy and medical applications. *Nucl* Data Sheets 2014;120:211–224.

[33] Meyer S, Bortfeldt J, Lämmer P, Englbrecht FS, Pinto M, Schnürle K, Würl M, Parodi K. Optimization and performance study of a proton CT system for pre-clinical small animal imaging. Phys Med Biol 2020;65(15):155008.

[34] Bortfeldt J et al.. Low material budget floating strip Micromegas for ion transmission radiography. *Nucl* Instrum Methods Phys Res 2017;845:210–224.

[35] Würl M, Englbrecht F, Parodi K, Hillbrand M. Dosimetric impact of the low-dose envelope of scanned proton beams at a ProBeam facility: comparison of measurements with TPS and MC calculations. *Phys* Med Biol 2016;61:958.

[36] Wang G, Jiang M. Ordered-subset simultaneous algebraic reconstruction techniques (OSSART). J X-Ray Sci Technol 2004;12:169–177.

[37] Penfold SN, Schulte RW, Censor Y, Rosenfeld AB. Total variation superiorization schemes in proton computed tomography image reconstruction. *Med* Phys 2010;37:5887–5895.

[38] Lowe David G. Distinctive Image Features from Scale-Invariant Keypoints. Int J Comput Vis 2004;60(2):91–110.

Please cite this article as: P. Palaniappan, Y. Knudsen, S. Meyer et al., Multi-stage image registration based on list-mode proton radiographies for small animal proton irradiation: A simulation study, Z Med Phys, https://doi.org/10.1016/j.zemedi.2023.04.003

[39] Rohlfing T. Image similarity and tissue overlaps as surrogates for image registration accuracy: widely used but unreliable. IEEE Trans Med Imaging 2012 Feb;31(2):153–163. https://doi.org/10.1109/TMI.2011.2163944.

[40] Paganelli C, Meschini G, Molinelli S, Riboldi M, Baroni G. Patient-specific validation of deformable image registration in radiation therapy: overview and caveats. Med Phys 2018;45(10):e908–e922.

[41] Gianoli C, Göppel M, Meyer S, Palaniappan P, Rädler M, Kamp F, Belka C, Riboldi M, Parodi K. Patient-specific CT calibration based on ion radiography for different detector configurations in 1H, 4He and 12C ion pencil beam scanning. Phys Med Biol 2020;65(24):245014.

Please cite this article as: P. Palaniappan, Y. Knudsen, S. Meyer et al., Multi-stage image registration based on list-mode proton radiographies for small animal proton irradiation: A simulation study, Z Med Phys, https://doi.org/10.1016/j.zemedi.2023.04.003